CrossMark

PAPER

Hydrological connectivity of alluvial Andean valleys: a groundwater/surface-water interaction case study in Ecuador

Pablo Guzmán[1,2,3] · Christian Anibas[1] · Okke Batelaan[1,4] ·
Marijke Huysmans[1] · Guido Wyseure[2]

Abstract The Andean region is characterized by important intramontane alluvial and glacial valleys; a typical example is the Tarqui alluvial plain, Ecuador. Such valley plains are densely populated and/or very attractive for urban and infrastructural development. Their aquifers offer opportunities for the required water resources. Groundwater/surface-water (GW–SW) interaction generally entails recharge to or discharge from the aquifer, dependent on the hydraulic connection between surface water and groundwater. Since GW–SW interaction in Andean catchments has hardly been addressed, the objectives of this study are to investigate GW–SW interaction in the Tarqui alluvial plain and to understand the role of the morphology of the alluvial valley in the hydrological response and in the hydrological connection between hillslopes and the aquifers in the valley floor. This study is based on extensive field measurements, groundwater-flow modelling and the application of temperature as a groundwater tracer. Results show that the morphological conditions of a valley influence GW–SW interaction. Gaining and losing river sections are observed in narrow and wide alluvial valley sections, respectively. Modelling shows a strong hydrological connectivity between the hillslopes and the alluvial valley; up to 92 % of recharge of the alluvial deposits originates from lateral flow from the hillslopes. The alluvial plain forms a buffer or transition zone for the river as it sustains a gradual flow from the hills to the river. Future land-use planning and development should include concepts discussed in this study, such as hydrological connectivity, in order to better evaluate impact assessments on water resources and aquatic ecosystems.

Keywords Groundwater/surface-water relations · Andean catchment · Hydrological connectivity · Temperature tracer · Ecuador

✉ Pablo Guzmán
   pguzmanc@vub.ac.be

[1] Department of Hydrology and Hydraulic Engineering, Vrije Universiteit Brussel, Pleinlaan 2, 1050 Brussels, Belgium

[2] Department of Earth and Environmental Sciences, KU Leuven, Celestijnenlaan 200e - bus 2410, 3001 Heverlee, Belgium

[3] Programa de Manejo de Agua y Suelo, PROMAS, Universidad de Cuenca, Cuenca, Ecuador

[4] National Centre for Groundwater Research and Training, School of the Environment, Flinders University, GPO Box 2100, Adelaide, SA 5001, Australia

Introduction

Surface water features like streams, lakes, reservoirs, wetlands and estuaries interact in many ways with groundwater. This process is commonly referred to as groundwater/surface-water (GW–SW) interaction. GW–SW interaction is an important group of hydrologic processes covering a wide range of spatial scales, from local scale (Woessner 2000; Sophocleous 2002) over river reach scale (Anibas et al. 2012) up to catchment scale (Amoros and Bornette 2002; Pringle 2003). In streams, this interaction is key to understanding recharge to or discharge from aquifers, dependent on the hydraulic connection between surface water and groundwater (Winter et al. 1999).

Since the aquifer and the stream form a continuum within a catchment (Holmes 2000), GW–SW interaction increases hydrological connectivity of water between different landscape components (Bracken and Croke 2007; Tetzlaff et al. 2007). The concept of hydrological connectivity emphasizes the importance of GW–SW interaction for understanding of hydrologic and hydrogeologic systems (Woessner 2000; Lane et al.

Springer

2004) as well as for hydro-ecological processes (Sophocleous 2002). Hydrological connectivity between the channel network and the surrounding hillslopes affects also the dynamics of runoff generation (Tetzlaff et al. 2007).

Specific models at both fluvial plain and reach scale are necessary to manage the water quality and sustainability of the connected surface and groundwater resources, the floodplain ecological functions (Woessner 2000) and for stream-restoration efforts (Sophocleous 2002; Soulsby et al. 2001); thus, a thorough understanding of GW–SW interaction is needed.

In riparian and hyporheic zones, GW–SW interaction is the major process for the continuous exchange of energy, oxygen, organisms and nutrients (Gibert et al. 1994; Smith 2005). Moreover, hyporheic exchange processes are thought to strongly influence the composition and behaviour of nutrients or pollution both in the groundwater system and in the stream (Brunke and Gonser 1997; Wroblicky et al. 1998). The stream water quality, hence, is highly influenced by the magnitude, direction and variation of exchange flows (Hancock et al. 2005; Pretty et al. 2006), which help to attenuate contaminants during low flow periods (Ellis et al. 2007). Differences found in biodiversity between sites dominated by discharging or recharging conditions (Datry et al. 2007) stress the importance for understanding GW–SW exchange processes. Extensive studies regarding flow, transport of nutrients, carbon, and oxygen between surface waters and groundwater were therefore developed for example by Wroblicky et al. (1998) and Dahm et al. (1998).

A wide range of techniques have been developed to quantify GW–SW interaction in its various spatial and temporal scales (Kalbus et al. 2006). These methods include the measurement of hydraulic head gradients, differential stream flow measurements, seepage meters and environmental tracers, including the use of heat as a groundwater tracer (Anderson 2005; Constantz 2008; Anibas et al. 2009). Most authors recommend a multi-scale approach combining different techniques to reduce the considerable uncertainties and to constrain flux estimates.

Hydrological research in the Andes is often focused on the evaluation of rainfall-runoff characteristics with a special interest in *páramos* (Buytaert et al. 2004; Buytaert and Beven 2011). Páramo is a neotropical grassland ecosystem predominant at high elevations, 3,500 m above sea level (a.s.l.; Buytaert et al. 2006). Baseflow in the rivers of Andean catchments has been linked to physical characteristics of páramos (Guzmán et al. 2015).

The soils on the steep Andes slopes are typically composed of shallow bedrock material. It is therefore often assumed that the aquifers have little importance in the hydrology of the Andes. However, there are substantial gaps in understanding the hydrological functions of shallow aquifers. GW–SW interaction in Andean catchments has not been studied yet.

A number of important inter-Andean alluvial plains are present. An example is the Tarqui alluvial plain, Ecuador. Many such plains occur in the inter-Andean depression and they are relatively densely populated. Considering that alluvial valleys are very attractive for future urban and infrastructural development, the study reported here is important in contributing to a better protection and/or management of the area and its water resources. It is hypothesized that the alluvial plain plays a crucial role in connecting the hillslopes with the stream.

Hence, the objectives of this study are to investigate GW–SW interaction in the Tarqui alluvial plain by means of extensive field measurements and by applying modelling tools like temperature as a groundwater tracer and groundwater flow modelling. The field measurements include investigations in groundwater heads across the alluvial plain, river stages, streambed temperatures and precipitation for more than 9 months. The spatial and temporal variations of this GW–SW exchange will be investigated and the contribution of the alluvial plain to the stream flow will be quantified. This study will help to better understand the larger Tarqui River system, and especially the impact of the morphology of the alluvial valley on the hydrological response and the hydrological connection with the stream.

Study area

The Andes in the south of Ecuador consists of a mixed landscape of fairly high and steep-sloped mountains with valleys in between them. The study area is situated in the Cumbe River Valley, one of the tributaries of the Tarqui River, part of the Paute catchment, which drains to the Amazon.

Geologically the western side of Tarqui consists of the north–south-oriented ridge called Western Cordillera and Tarqui formation. Western Cordillera is formed by sedimentary and basic to intermediate volcanic deposits from the Cretaceous and the early Tertiary (Barberi et al. 1988). Tarqui formation is late Miocene to Plio-Pleistocene, which includes rhyolitic to andesitic volcanic breccias, pyroclastic flows, ignimbrites, and airborne tuffs (Hungerbühler et al. 2002). Tarqui formation forms the eastern side of the catchment. The central depression of Tarqui is formed by alluvial deposits (Plio-Pleistocene fluviatile and lacustrine volcanoclatic deposits). There is a fault oriented south–north following the direction of Tarqui River. Orogenesis exposed the emerging ridges to pyroclasts and Plio-Pleistocene fluviatile and lacustrine deposits filled the interandean depression. The upper parts of the Cordilleras, the older Palaeozoic basements, were exposed by erosion. The layers below andosols in the upper catchments have very low permeability due to the glacial compaction suffered during the Tertiary.

The functioning of the Tarqui alluvial valley with regard to the stream flow and riparian ecology is largely unknown; the

lack of data still is a major challenge. During the 1980s and 1990s, the Tarqui River alluvial plain was severely altered by straightening meanders and the construction of drains. As a consequence, fluviomorphological problems have appeared along the stream. Sallow trees, for example, died at the river banks. The specific hydrological and ecological effects and the impact of the changed GW–SW interaction patterns remain unclear. The same is valid for future impacts on river flows, aquatic ecology and GW–SW interaction due to (sub-)urban sprawl in the catchment and its amenity for infrastructural development. The alluvial plain of the Tarqui River is considered as site for a future airport for the city of Cuenca, with all its potential morphological and hydrogeological impacts.

For studying GW–SW interaction, the catchment of the Cumbe River offers suitable conditions. It is feasible to measure water tables, stream levels and discharges, and streambed temperatures with limited resources. The landscape configuration formed by a combination of hillslopes and an alluvial plain is of special interest for studying the hydrological behaviour of the alluvial plain.

The outlet of the Cumbe River (Fig. 1) is located approximately 16 km south of the city of Cuenca, between the coordinates UTM (WGS84, zone 17 south): 716,450 and 722,965 UTMx; and 9,649,137 and 9,665,556 UTMy. The Cumbe

Fig. 1 The Cumbe River catchment, located in the central south of Ecuador. The catchment is part of the Tarqui River catchment

River catchment has a size of about 56 km^2 and the elevation ranges from 2,600 to 3,480 m a.s.l. with a mean of 2,953 m a.s.l. The valley is 2–3 km wide in the south–north direction. A digital elevation model (DEM) with 5×5 m spatial resolution provides the topographic details (Fig. 1). The slope in the Cumbe catchment varies from 0 to 65° with a mean slope of 17.8°.

The annual temperature is 14 °C and the estimated precipitation is 820 mm/year. According to a satellite image classification acquired in 2010 (Broekaert 2012), land use in Cumbe consists of grassland (38.1 %), arable land and urban area (26.9 %), forest (23 %), páramo 7.5 % and degraded land 4.4 %.

Since the hillslopes are covered by shallow soils on steep slopes, surface runoff is the predominant response, more than lateral interflow. During the fieldwork it was observed that many small streams show a gradually diminishing flow downslope and that many run dry at the foot of the hillslope before reaching the alluvial plain. This indicates that these streams are losing and do recharge the alluvial aquifer. Also, the small streams from the hillslopes do not cross-cut the alluvial plain towards the main river. The vertical groundwater recharge in the alluvial plain occurs over an area characterized by flat topography.

The alluvial plain of Cumbe consists of several layers of sediments. There are two different sources for sediments in the alluvial plains: the first one is linked to hillslope erosion and sediment deposition at the foothills and the second originates from river flooding. Thicker intercalated layers of fine sand and clay were found close to the foot hills while thin layers of mixed materials are observed close to the River. A major road parallel to the river runs on the east side of the valley. Artificial ditches and infrastructure have also changed hydrological connections.

Materials, methods and data

Groundwater heads and river stages

Seven piezometers with pressure transducers (Schlumberger DI501-Diver and DI500-Baro) for measuring groundwater levels and water temperature were installed across the alluvial plain perpendicular to the Cumbe River (Fig. 1). Figure 2 shows the layout and obtained water levels of the installed P1–P7 piezometers and Table 1 records their main characteristics. The piezometers are constructed with PVC pipes, in two parts, a blind and a perforated section. The perforated section is covered by a geotextile and surrounded by sand; at the top, the surface around the piezometer has been sealed with cement.

The river level was measured in a concrete trapezoidal flume. The flume is 3.1 m wide on the top, 1.17 m high and
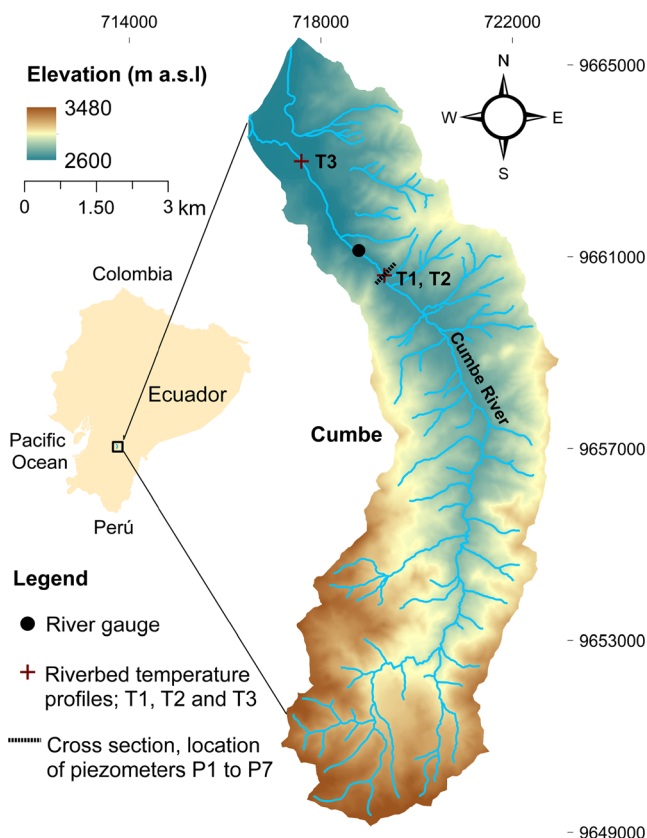
Fig. 2 Location and measured water levels of piezometers *P1–P7*, in the cross section perpendicular to the Cumbe River. In general, the water level becomes shallower towards the river, while the absolute water level is higher towards the hill slope. The distances are measured from the Cumbe River: positive distances for piezometers located west and negative for piezometer *P7* located to the east side of the River. P5 and P6 are located between *P4* and the river
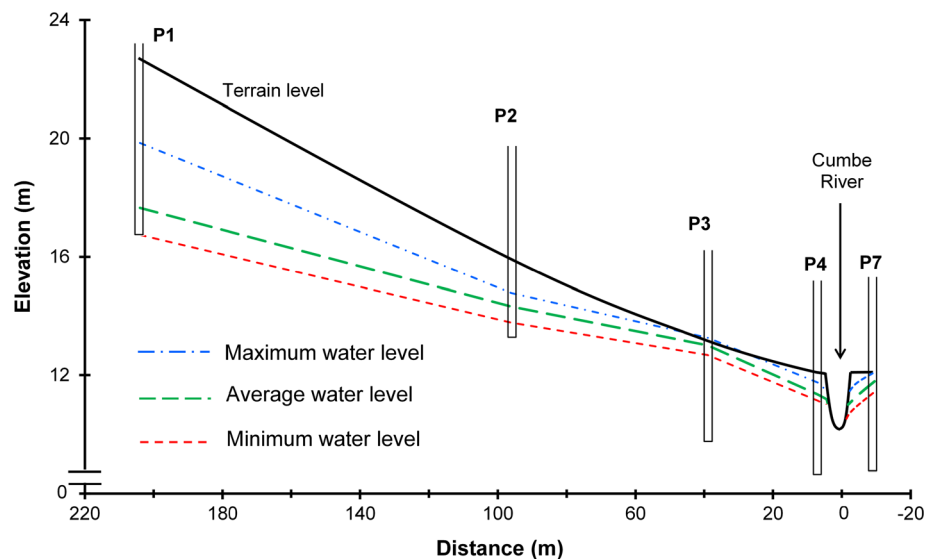
0.5 m bottom wide. Water level data are available from June 10, 2011 till August 23, 2013 (805 days) and from June 1, 2011 till December 13, 2012 (553 days) for groundwater heads and river stages respectively. The data series of P2 and P7 showed 10 and 17 % of gaps respectively, which was caused by problems with the sensors.

For convenience, the reference elevation at 2,633.45 m a.s.l. has been selected in this study, which is 10 m below the river-bed, and this study has expressed all water levels in meters relative to this reference. The terrain levels and references were accurately measured by a dumpy level.

Slug tests applying the inversed auger-hole method (Ritzema 1994) were performed in piezometers P1–P7 (Fig. 2) to estimate horizontal hydraulic conductivity. Changes in water table were measured in a time interval of 5 s using the pressure transducers installed in each piezometer. The hydraulic conductivity is estimated by the Eq. (1), based on the Darcy law:

$$K = 1.15\, r\, \frac{\left[\log\left(h_1 + \frac{r}{2}\right) - \log\left(h_2 + \frac{r}{2}\right)\right]}{t_2 - t_1} \quad (1)$$

Where K is the horizontal hydraulic conductivity in m/d, r (m) is the radius of the well, h_1 and h_2 hydraulic heads in m, these measured at time step t_1 and t_2 respectively.

The uncertainties in the measurements are related to the fact that the measurements of water levels during the slug tests provide values for only a small support volume surrounding the piezometer; thus, the estimated hydraulic conductivity is mostly representative of this portion of the aquifer. The soil layers in the alluvial plain have different hydraulic conductivities which affect the hydraulic head (h_1 and h_2), and hence the results of Eq. (1).

Vertical temperature profiles

Time series of vertical temperature profiles in the Cumbe River have been measured at three locations (Fig. 1). Two locations (T1 and T2) are aligned with the transect for measuring groundwater levels and a third (T3) is 2.4 km downstream in a wider section of the alluvial valley and close to the confluence with the Tarqui River. Since long-term measurements have been conducted, one issue during the development

Table 1 Characteristics of the piezometers installed in the alluvial plain of Cumbe

Piezometer location				Depth (m)	Diameter (cm)
ID	UTMx (m)	UTMy (m)	Ground elevation (m a.s.l.)		
P1	718,868	9,660,800	2,656.2	6.0	9.70
P2	718,908	9,660,900	2,649.4	2.7	7.30
P3	718,934	9,660,951	2,646.6	3.4	9.70
P4	718,954	9,660,977	2,645.5	3.4	9.70
P5	718,956	9,660,979	2,645.5	3.5	7.70
P6	718,959	9,660,980	2,643.5	2.5	7.70
P7	718,960	9,660,992	2,645.5	3.3	9.70

of this research was to install the equipment in suitable places where vandalism could be avoided. Location of T2 and its adjacent alluvial plain where the piezometers (P1–P7) are installed accomplishes the security conditions and provides easy access for constant monitoring and maintenance. At T3 the devices are located hidden below a small bridge. Only temperature was measured at T3 because it was logistically difficult to manage measurements at two locations, and there were no strong differences expected between the two sites (T2 and T3) anyway.

Vertical temperature profiles are determined using Onset UTBI-001 temperature data loggers, which were fixed to a steel rod at depths of 0.1, 0.2, 0.3, 0.5 and 1 m in the riverbed (Fig. 3).The rigidity of this system guarantees that the temperatures are always measured at the same depth. The right side of Fig. 3 shows the PVC perforated pipe which envelops the steel rod. At the top of the steel rod a steel cable has been fixed, which helps to recover the rod during the measurement campaigns.

The temperature loggers are fixed in such a way that there is no direct contact with the iron elements, to avoid disturbances in the measured temperature. Among the devices are sponges located to avoid risk of higher flow inside the tube caused by the lessening of resistance regarding to the surrounding alluvial material. Temperatures were recorded every 15 min, from February 2013 till December 2013 (326 days). The temperature in the stream is measured at 10 cm depth below the water surface, whereby the sensor is connected to a float that is kept at 10 cm below the surface.

Precipitation

Precipitation data were obtained from an existing weather station, which is administrated by the water company of the city of Cuenca. A time series of precipitation from 1998 till 2013 was available from a station located close to the confluence of the Cumbe and Tarqui rivers, 4 km downstream from the studied alluvial plain (UTMx (m) = 716,525; UTMy (m) = 9,

Fig. 3 Schematic set up for temperature measurement of vertical riverbed profiles at Cumbe River. Temperature data loggers are fixed to a steel rod at depths of 0.1, 0.2, 0.3, 0.5 and 1 m
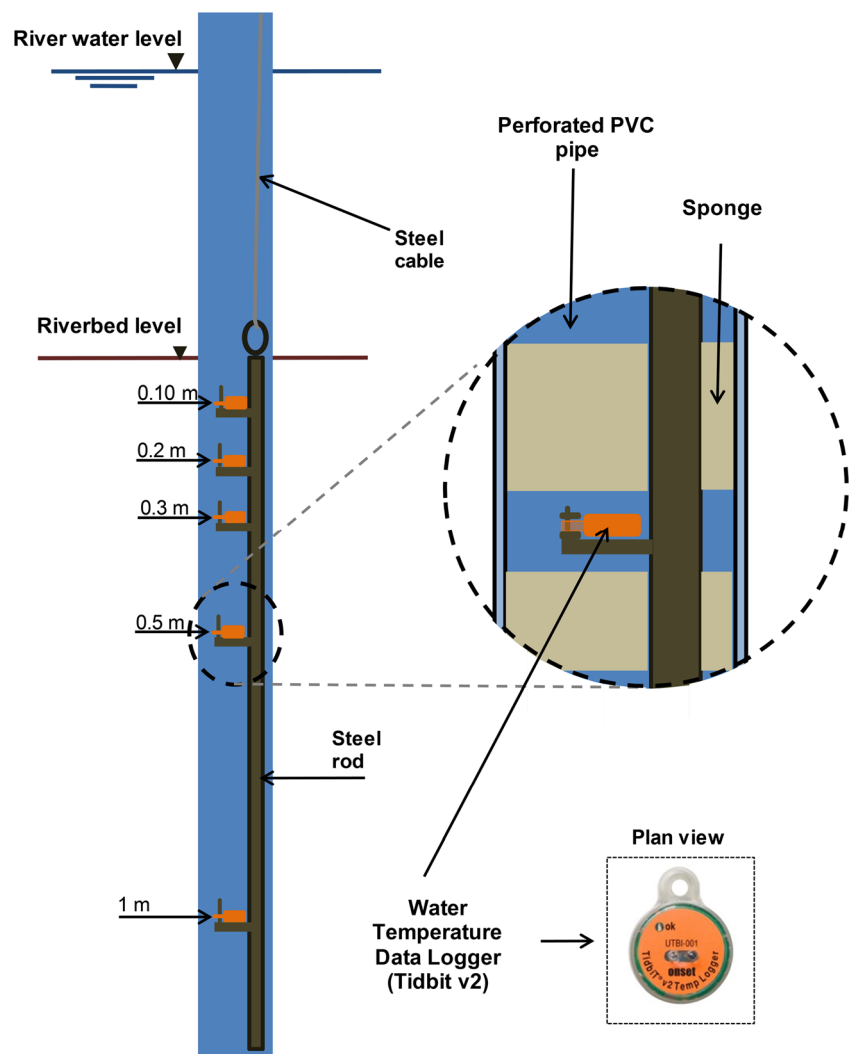
663,955; elevation = 2,630 m a.s.l.). Average monthly precipitation is presented in Fig. 4.

Groundwater/surface-water interaction modelling

Hillslope contribution and recharge assessment

The hillslope contribution and groundwater recharge to the alluvial plain aquifer of the Cumbe River have been quantified by calibrating a WetSpa model. WetSpa stands for Water and Energy Transfer between Soil, Plants and the Atmosphere. It is a physically based hydrologic model, developed in the Vrije Universiteit Brussel (VUB), Belgium (Wang et al. 1996; Liu and De Smedt 2004). It is integrated in a geographic information system (GIS) environment, and is capable of predicting the outflow hydrograph at the catchment outlet or any converging point in a watershed at variable time steps (De Smedt et al. 2000). WetSpa calculates in each grid cell the processes of precipitation, evapotranspiration, interception, surface runoff, soil moisture storage, interflow, recharge, groundwater storage and discharge as well as water balance in the root zone (Liu and De Smedt 2004).

The WetSpa model was calibrated for the entire Tarqui catchment using the daily discharge series at the outlet of the catchment.

Figure 5 shows WetSpa simulations of the hydrological system for each grid cell with four control volumes: the plant canopy, the soil surface, the root zone, and the saturated aquifer.

Digital maps of topography (DEM), soil, land-cover and meteorological data deliver the spatially distributed parameters for calculations at cell level. Liu and De Smedt (2004) present the equations used for the different water balance components at cell level. The Tarqui catchment is modelled using a pixel cell size of 30 × 30 m.
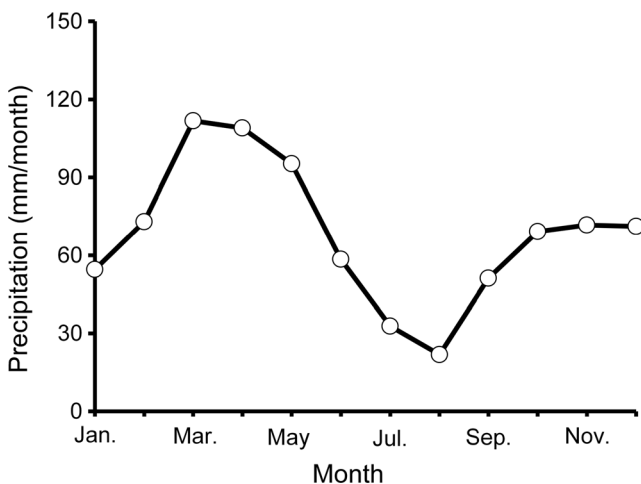

Fig. 4 Average (1998–2003) monthly precipitation for the lower Cumbe River catchment showing a bimodal pattern: March to April receives more rainfall, while June to August are the drier months

WetSpa produces distributed maps of recharge and runoff. Runoff is infiltrating into the streambed and recharging the alluvial aquifer; therefore, the hillslope contribution from the runoff is calculated by WetSpa. The area that drains into the studied area from the west and east hills is estimated to be 0.284 and 0.127 km² respectively. WetSpa estimated values of recharge and hillslope runoff, which are used in the groundwater modelling as starting values and later as lower and upper limits for the boundary conditions during the calibration of the hillslope contribution and recharge into the alluvial valley.

Groundwater flow model

The exchange fluxes between the aquifer and the river are quantitatively assessed by modelling groundwater flow in the alluvial plain of Cumbe River. A fully distributed, steady-state groundwater flow model was built in MODFLOW 2000 (Harbaugh et al. 2000; Harbaugh 2005) via the GUI Processing MODFLOW 8 (PMWIN 8; Chiang and Kinzelbach 1998).

The main components of recharge in the alluvial plain are the west and east runoff infiltration and the recharge on top of the alluvial plain. These components of recharge are estimated from the WetSpa fully distributed hydrological model calibrated for the Tarqui catchment. The periods for calibration and validation of the hydrological model were respectively from October 24, 1998 to June 21, 2001 (972 days) and from June 10, 2009 to August 14, 2011 (796 days), both different from the ones used in the groundwater flow model.

The alluvial plain of Cumbe River contains intercalated sedimentary layers of fine and coarse materials. This heterogeneity likely creates spatial differences in the lateral groundwater movement towards the river.

The hydraulic conductivity in this study is assessed by field measurements in specific piezometers, thus it is difficult to capture the heterogeneity of hydraulic conductivity in the alluvium and, hence, the uncertainty in the measured values is high. The same is true for other model parameters where no or only limited amounts of direct measurements are available. Due to the uncertainties, a steady-state model aimed at capturing the average characteristics of the alluvial plain is established. However, the steady-state model has been set up for seven different periods in order to cover temporal variation of GW–SW interaction.

The groundwater flow model consists of an unconfined layer which is 275 m long and 160 m wide with grid cells of 10 × 10 m. The width of the model represents the part of the alluvial plain where the piezometers have been installed. The east and west boundaries are constant flow boundaries representing the flow from the hillslopes, while the land use (pasture) and the characteristics of the soils are considered homogeneous due to topography characteristics (flat area with the main slope towards the river). Cells are refined to 2 × 10 m
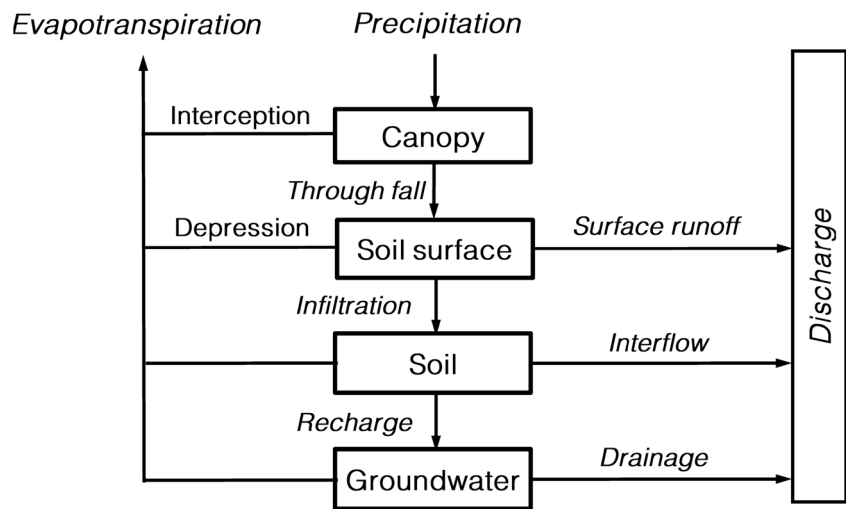
close to the river. The north and south boundaries are no flow boundaries, as groundwater flow in the south–north direction is expected to be negligible due to the morphological characteristics and head gradients. A constant recharge boundary is applied at the top of the model.

The MODFLOW River package is used along the Cumbe River for quantifying the GW–SW interaction (Fig. 6). The hydraulic conductance of the riverbed is calculated with:

$$C_r = \frac{K_r \, L \, W_r}{M_r} \qquad (2)$$

where K_r (m/d) is the hydraulic conductivity measured in piezometer P6, which is located in the riverbed close to the riverbank; L (m) is the river length; W_r the width of the river (2.5 m); and M_r the thickness of the riverbed (0.8 m) as assessed from

field observations. The elevation of the riverbed bottom is 10 m above to the reference elevation at 2,633.45 m a.s.l.

Flow from the hillslopes is estimated based on the contributing area that drains towards the east and west boundaries as previously explained (Fig. 6). Since it was not possible to establish specific variations of the recharge during the periods of groundwater flow simulation, average conditions for recharge were assumed. An overview of initial values of the parameters related to the different boundary conditions is presented in Table 2.

Along the alluvial plain, the horizontal hydraulic conductivity has been zoned into four regions based on the hydraulic conductivity data obtained by slug tests (Fig. 6). Hydraulic conductivities at K1–K4 are expected to represent the heterogeneity of sediment layers across the alluvial plain; thus, close to the western foothill, the sediments originate from erosion
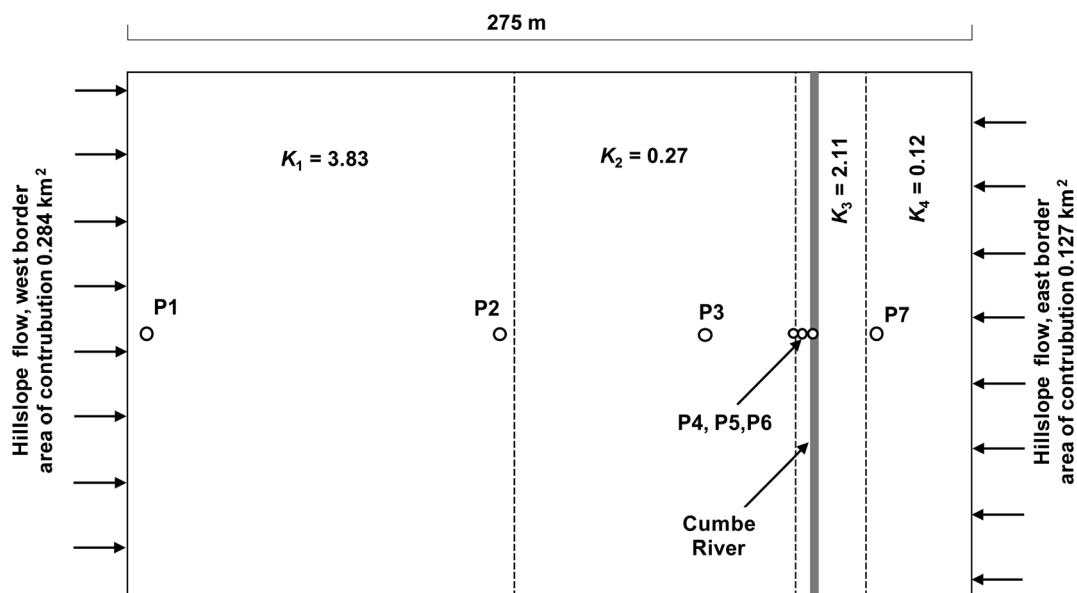

Fig. 6 Conceptual groundwater flow model of the Cumbe alluvial plain. K_1–K_4 represent horizontal hydraulic conductivity (m/d) at sites $K1$–$K4$

Table 2 Initial values of parameters related to the boundary conditions

Parameter	Value
Recharge (m³/d)	10
Hillslope flow (west side) (m³/d)	101
Hillslope flow (east side) (m³/d)	45
River hydraulic conductance (m²/d)	906

and deposition (fine sand and clay); towards the river, the sediments are predominantly those that originate from fluvial deposition; near the river channel, there is coarser material and lime; and at the eastern foothill, a combination of fine materials is found.

The morphological conditions and piezometric levels in the study area indicate groundwater flow from the aquifer to the river. Measured hydraulic heads in P1–P7 (Fig. 3; Table 3) are used to calibrate the groundwater model. Four horizontal hydraulic conductivities (Fig. 6), the recharge over the alluvial plain, and the flow from the western and eastern hillslopes are calibrated. The parameter estimation module PEST (Watermark 2004) was used for automatic calibration of these parameters. Maximum and minimum values for calibration of hydraulic conductivity are specified considering soil structure and heterogeneity observed during field visits; therefore, hydraulic conductivity at K1 ranges from 0.5 to 5 m/d, and at K2, K3 and K4 ranges from 0.02 to 3 m/d. The calibration of the hillslope contribution and recharge into the alluvial valley is constrained by maximum and minimum values obtained from the WetSpa simulation.

For establishing temporal variations in GW–SW interaction, periodical changes of head and river stages along the data series have been considered. Seven different periods (i.e. 1–7) were identified by analysing variations of water levels in P1, which exhibits the largest variation in hydraulic head.

Periods were identified where hydraulic head is consistently above or below the average hydraulic head in P1. Periods characterized by low hydraulic head yield hydraulic head values of, respectively, 0.64 m (September– December

2011), 0.57 m (May–July 2012) and 0.58 m (October 2012– May 2013) below the average in P1. The highest average hydraulic head is 0.89 m (December 2011–May 2012) above the average in P1. Periods with moderately high hydraulic head yield hydraulic head values of 0.32 m (June– September 2011), 0.28 m (July–October 2012) and 0.27 m (May–August 2013) above the average in P1.

Temperature as a groundwater tracer for vertical flux assessment

Although groundwater flow is driven by hydraulic gradients, heat in the subsurface is transported by advection with the groundwater flow, and heat conduction is driven by temperature gradients. Groundwater flow therefore influences the temperature distribution in aquifers and hyporheic zones below and beside rivers and streams; thus, heat can be used as a groundwater tracer (Anderson 2005). As a measure of heat, temperature data can be acquired cost-effectively and with a high temporal resolution using combined sensor-logger units. These items are now widely available and can be handled easily (Fig. 3).

Based on Stallman (1965) and Lapham (1989), the vertical 1D, anisothermal transport of water and heat through homogeneous porous media is formulated as:

$$\rho c \frac{\partial T}{\partial t} = \kappa \frac{\partial^2 T}{\partial z^2} - q_z \rho_w c_w \frac{\partial T}{\partial z} \tag{3}$$

with

$$\rho c = n\rho_w c_w + (1-n)\rho_s c_s \tag{4}$$

and

$$\kappa = n\kappa_w + (1-n)\kappa_s \tag{5}$$

where k is the effective thermal conductivity of the soil-water matrix in J/(s m K), T the temperature at point z at time t in °C, $\rho_w c_w$ the volumetric heat capacity of the fluid in J/(m³K), q_z

Table 3 Characteristics of data series of groundwater heads (from June 2011 till August 2013) and river stages (from June 2011 till December 2012) as well as horizontal hydraulic conductivity (m/d). High values are observed in piezometers *P1* and *P2* (located close to the foot of the hillslope) and piezometer *P6* (in the west bank of Cumbe River)

Measurement point	Average water level (m)	Minimum water level (m)	Maximum water level (m)	Level range (m)	Horizontal hydraulic conductivity (m/d)
P 1	17.65	16.74	19.85	3.11	4.26
P 2	14.31	13.77	14.77	1.00	3.39
P 3	13.00	12.68	13.26	0.58	0.05
P 4	11.34	11.13	11.75	0.62	0.49
P 5	11.18	10.99	11.47	0.48	1.40
P 6	10.17	10.00	10.71	0.71	2.83
P 7	11.70	11.37	12.05	0.68	0.12
River stage	10.65	10.49	11.22	0.73	–

the vertical component of the groundwater velocity in m/s, ρc the volumetric heat capacity of the rock-fluid matrix in J/(m^{3}K). n is the dimensionless porosity, $\rho_s c_s$ the volumetric heat capacity of the solids in J/(m^{3}K) and , k_w, k_s are respectively the thermal conductivities of water and the solids [J/(s m K)]. The first term on the right hand side of Eq. (3) represents the conductive and the second term the advective part of the transport.

The temperature data measured in the field are processed with a heat transport model in order to derive quantitative estimates of the fluxes. Therefore inverse modelling has been applied in which the calculation of vertical groundwater fluxes is achieved by solving Eq. (3) with transient boundary conditions using STRIVE (Anibas et al. 2009, 2012).

STRIVE is a numerical, vertical one-dimensional (1D) water flow and heat transport model based on the ecosystem modelling platform FEMME (Soetaert et al. 2002), which was successfully applied in different hydrogeological settings, including sandy riverbeds (Anibas et al. 2008, 2011) and riverbeds composed of organic soils (Anibas et al. 2012). STRIVE estimates the value of q_z by minimizing the difference between the measured and simulated temperature distributions by user-defined internal integration and fitting routines (Soetaert et al. 2002).

The STRIVE model for the Cumbe River was discretized as a vertical 1D homogeneous saturated soil column of 5.0 m depth composed of 100 layers with unequal spacing. This provides thin layers of 0.001 m at the upper boundary, where most temperature changes occur, whereas the thickness of the layers is increasing towards the centre of the model domain to 0.08 m.

The necessary input parameters for STRIVE were based on field examinations at sites T2 and T3. The riverbed was characterized as sand and silty sand respectively. Porosity, density and thermal conductivity of solids are estimated from literature and heat capacity by the empirical equation of De Vries (1963). Thus, for locations T2 and T3, the porosity is 0.47 and 0.46, and the heat capacity of the solids c_s [J/(kg K)] is 697 and 696, respectively; the density of the solids ρ_s [kg/m^3] for both T2 and T3 is 2,650, and the thermal conductivity of the solids k_s [J/(s m K)] for both is 2.90. The heat capacity of water c_w is 4,180 J/(kg K), density of water ρ_w is 1,000 kg/m^3 and thermal conductivity of water k_w is 0.60 J/(s m K).

While at the upper model boundary, the uppermost temperature time series is applied, the lower model boundary at 5.0 m depth is defined by a constant temperature of 16 °C. This temperature represents the average groundwater temperature of the area and is calculated from the temperature measured in the piezometers (P1–P7). The other temperature time series are used to fit the simulated temperatures to the measured ones.

Results and discussion

Measured water levels

Table 3 summarizes the main characteristics of water heads and river stages measured at the Cumbe River. The range expresses the difference between maximum and minimum water level. In order to fill the data gaps in piezometers P2 and P7, and to complete the river stage series, the correlation between data series of piezometer P6 and river stage, between piezometers P6 and P7, and between piezometers P1 and P2, has been analysed.

There is a good linear correlation between piezometer P6 and the river stage (Fig. 7a; $R^2 = 0.73$), a poor correlation between piezometers P7 and P6 ($R^2 = -0.282$), and good non-linear correlation among piezometers P1 and P2 (Fig. 7b; $R^2 = 0.70$). The river stage series were completed and filled the gaps of piezometer P2 by using the equations described in Fig. 7.

The observed water level variations support the conceptual model of Fig. 6, as P1 and P7 are exposed to greater water level variations due to aquifer recharge from runoff and interflow that infiltrates from the hillslopes. Water level in piezometer P7 varies less than in P1 due to the smaller hillslope contributing area and the presence of the road infrastructure, which affects the recharge and interflow (Figs. 2 and 6). The maximum range of water level variations is registered in P1. This is an indication of the influence of surface runoff from the nearby hillslope. It results in recharge events by infiltration at the foot of the hillslope and consequently increases water level.

Vertical temperature profiles

During the observation period from February 2013 till December 2013, the average river temperature was around 14 °C, and the range was 10 °C. The average temperature at 1 m below the surface at T1 was 16 °C with a range of 0.9 °C; T2 and T3 show an average temperature of 14.8 and 14.4 °C, respectively, with a range of 2.6 and 2.9 °C. The measured temporal and spatial variation of temperature along the profile at T1 to T3 is shown in Fig 8.

Temperatures measured at T1 (riverbank location, Fig. 8a) exhibit little variation along the profile; the temperature along the profile is of the groundwater and is more or less constant at 16 °C. Thus, it is assumed that groundwater and surface water are disconnected and the flow of water is prominently lateral rather than vertical, which is highly plausible based on the morphological configuration of the studied area.

The measured variation of temperature of the Cumbe River at T2 and T3 is similar and relatively high, ranging from 10 to 20 °C (Fig. 8b,c). This variation is mostly linked to environmental temperature variations of the land surface. At T2
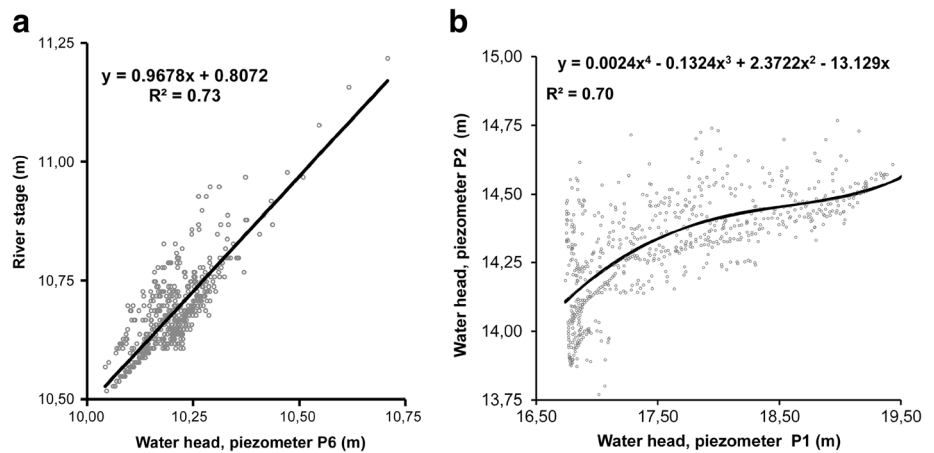
(Fig. 8b), immediately below the riverbed at 0.1 m depth, the temperature becomes more stable indicating an upward flux (from the aquifer to the river) or a gaining stream (Constantz 2008). At T3 (Fig. 8c), the temperature throughout the soil profile remains highly variable, decreasing considerably just below 0.5 m. This penetration of temperature-variation in the soil profile is an indicator of downward exchange flux (from the river to the aquifer) or losing stream (Constantz 2008).

Groundwater modelling, hillslope flow contribution and groundwater/surface-water interaction

The comparison between observed and calculated hydraulic heads, using the starting parameter estimates as given in Table 2 and Fig. 6, resulted in a root mean square error (RMSE) and variance of 0.96 and 0.93 m^2 respectively. Starting with this parameter set, the variance was minimized by calibrating the MODFLOW model.

The resulting optimized values of horizontal hydraulic conductivity are shown in Table 4. The relative composite sensitivities of hydraulic conductivity and the limits of the 95 % confidence interval are shown as well. The relative sensitivity is a measure of the changes in model outputs that are incurred by a change in the value of the parameter (Watermark

2004).The 95 % limit of confidence shows that horizontal hydraulic conductivity at K4 is the least sensitive and is therefore estimated with a very large margin of uncertainty. The values at K1, K2 and K3 show low uncertainty, with K1 and K2 being more sensitive than K3 (Table 4).

The calibrated horizontal hydraulic conductivities in Table 4 moderately differ from the values obtained from the field measurements except for K3 which changes two orders of magnitude (Fig. 5). K3 could be influenced by the presence of organic material combined with fine sediments deposited in the river channel. Alluvial aquifers can display a very heterogeneous hydraulic conductivity (K) with values varying over several orders of magnitude. Moreover, the K values obtained by slug tests represent mainly horizontal hydraulic conductivity of only a shallow part of the alluvial aquifer. The presence of lenses or layers of fine material (clay) could influence the values at K1 and K2. The Cumbe River furthermore receives deposits of the sewage system of the small population of Cumbe contributing to the heterogeneity of the riverbed hydraulic conductivity.

Once the hydraulic conductivities were calibrated, the western and eastern hillslope flows and the recharge were calibrated for the seven periods. The GW–SW interaction is determined from the groundwater flow model. A hydrological

Fig. 8 Box plots for vertical temperature profiles at the Cumbe River. **a** Temperature profile T1, showing no vertical exchange. **b** Profile T2 and **c** profile T3 show upward and downward exchange, respectively
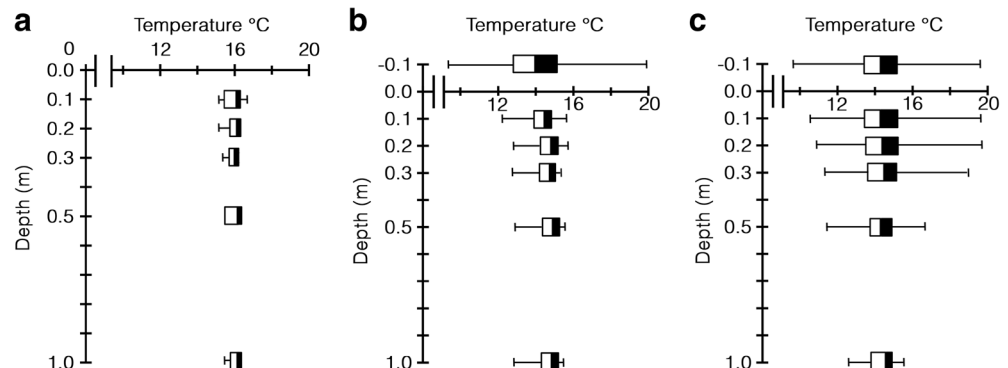
Table 4 Calibrated horizontal hydraulic conductivity values. Higher values are shown for *K1* and *K2*, whereas *K3* has a lower value

Site	Calibrated value (m/d)	Relative sensitivity	95 % confidence limits	
			Lower limit (m/d)	Upper limit (m/d)
K1	0.61	0.636	0.46	0.80
K2	0.89	0.754	0.63	1.26
K3	0.07	0.066	0.05	0.09
K4	0.21	0.004	2.1E-06	2.0E+4

conceptual model (Fig. 9) in the form of a schematic cross section was developed (from field observations, data analysis and previous studies) and exhibits the results for average west and east hillside flows (runoff infiltration), recharge and GW–SW interaction. It corresponds to the location of the cross section shown in Fig. 1.

Table 5 exhibits the results and variation of the components presented in Fig. 9 for different periods of time and Table 6 provides the 95 % limits of confidence interval for hillslope flow and recharge. In Tables 5 and 6, the seven periods of time (i.e. 1–7) are; "1" from June to September 2011, "2" from September to December 2011, "3" from December 2011 to May 2012, "4" from May to July 2012, "5" from July to October 2012, "6" from October 2012 to May 2013, and "7" from May to August 2013.

The calibrated western hillslope flows show lower uncertainty, and on average the flow is 76 % of the GW–SW exchange (river leakage). The western hillslope flow differs on average 6 % from the hillslope flow estimated with the WetSpa model (Table 2). It slightly changes from period to period but it shows agreement with high and low hydraulic head in piezometer P1.

The eastern hillslope flow exhibits a larger margin of uncertainty than the western flow and on average it represents 16 % of the GW–SW exchange (river leakage). At any time it shows lower values than the WetSpa model estimated value, –

49 % on average, which can be explained by the presence of the road infrastructure located between the river and the eastern hillslope (Fig. 8). This infrastructure interrupts the natural pattern of flow due to changes of soil structure and drainage.

The recharge presents the largest uncertainty; however, the calibrated recharge in any period remains in the range of the values estimated with the WetSpa model. It is on average 8 % of the GW–SW exchange (river leakage), but fluctuates between periods. Low and high recharge values coincide with periods of lower and higher piezometric levels. The estimated recharge contribution to GW–SW exchange is 3, 4 and 1 % for periods 2, 4 and 6, and 10, 15, 14, and 12 % for periods 1, 3, 5, and 7.

The uncertainty, given by the 95 % confidence limits for hillslope flows (Table 6), shows agreement with the uncertainties for hydraulic conductivity (Table 4), thus lower uncertainty on the western side of the river and higher on the eastern side.

In Table 5 the negative sign in GW–SW interaction (river leakage) indicates flow from the aquifer to the river, i.e. gaining conditions. GW–SW interaction varies similarly to recharge and flows from the western hillslope (Table 5): high values in periods 1, 3, 5 and 7 and low values in periods 2, 4 and 6. The average river leakage for the seven periods is –141 m^3/d. Figure 10 shows a comparison between calculated and observed water heads
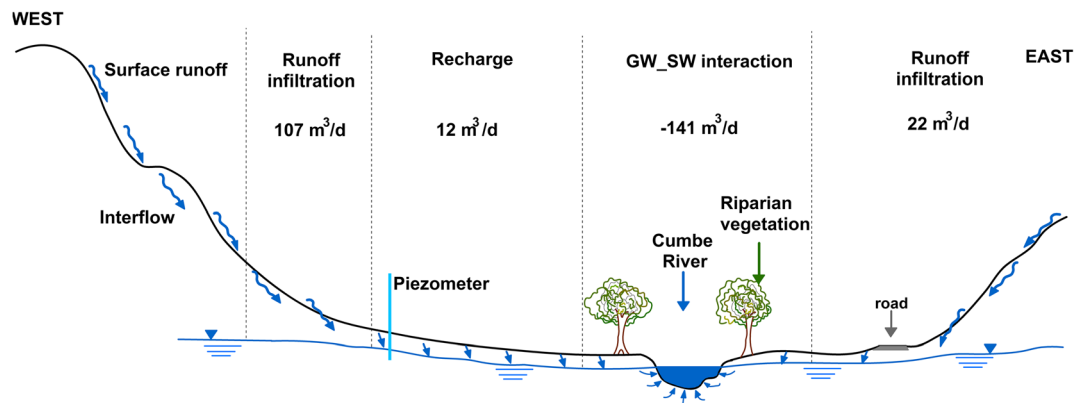

Fig. 9 The conceptual model of the Cumbe River catchment shows the results in a cross section spanning from the western to the eastern hillslopes. *Negative sign* indicates flow from the aquifer to the river

Table 5 Calibrated values of hillslope discharges and recharge considering steady state conditions and GW–SW interactions calculated with the MODFLOW model assessed for different time periods

Period	West hillslope flow (m³/d)	East hillslope flow (m³/d)	Recharge (m³/d)	GW–SW interaction (River leakage) (m³/d)
1	109.44	19.36	14.48	−143
2	103.84	22.88	3.56	−130
3	111.52	18.72	22.40	−153
4	102.56	20.16	4.71	−127
5	107.68	27.84	21.52	−157
6	105.12	22.24	0.97	−128
7	108.80	23.36	17.20	−149

before and after calibration. After calibration the variance of observed versus calculated hydraulic heads shows a considerable improvement.

Estimated GW–SW interaction using vertical temperature profiles

Vertical fluxes assessed with STRIVE confirm what is suggested by the box plots of temperature data in Fig. 7. At T2 water flows from the aquifer to the river, while at T3 a flux from the river towards the aquifer is indicated. The calibrated flows from MODFLOW in the area around T2 show the same behaviour as calculated with STRIVE.

The maximum estimated vertical fluxes calculated with the STRIVE model are –0.30 m³/d (T2) and 0.35 m³/d (T3) per meter of river for gaining and losing conditions, respectively. Both values occurred for May 2014. The average estimated vertical fluxes calculated with the STRIVE model for the whole period are – 0.20 m³/d (T2) and 0.09 m³/d (T3) per meter of river length for gaining and losing conditions respectively. The variation in time of vertical fluxes at T2 and T3 is presented in Fig. 11, which also includes accumulated precipitation.

At T2, the highest flux is found in months with high precipitation, while the lowest fluxes are indicated in October after a period of lower precipitation. An increasing flux tendency is observed from March to May. Fluxes close to the average (–0.20 m³/d/m) are found in the months of June to September. After October, an increasing tendency is shown. The behaviour at T2 is explained by the proximity of the hillslopes to the river. The main inflow in the alluvial aquifer is lateral hillslope-flow which depends directly on precipitation; therefore, the GW–SW exchange fluxes are linked to recharge by precipitation.

At T3, GW–SW interaction is mainly from the river to the aquifer. In September and October, a change in flow direction is identified as upward fluxes are observed. Due to the location of T3 there is a lower contribution from lateral hillslope-flow and the storage in the wider alluvial valley is much larger.

The prevalent flow direction from the river to the aquifer at T3 indicates a higher river stage than water level in the aquifer. River stages at T3 are mostly the product of upstream conditions. The precipitation tendencies around T3 do not always coincide with river stage changes; it can be seen in Fig. 11 that during the high precipitation of March there is relatively low flux. The exchange at T3 during the month of October suggests the precipitation affected mainly the recharge in the aquifer,

Table 6 95% limits of confidence interval for hillslope flow and recharge for different time periods

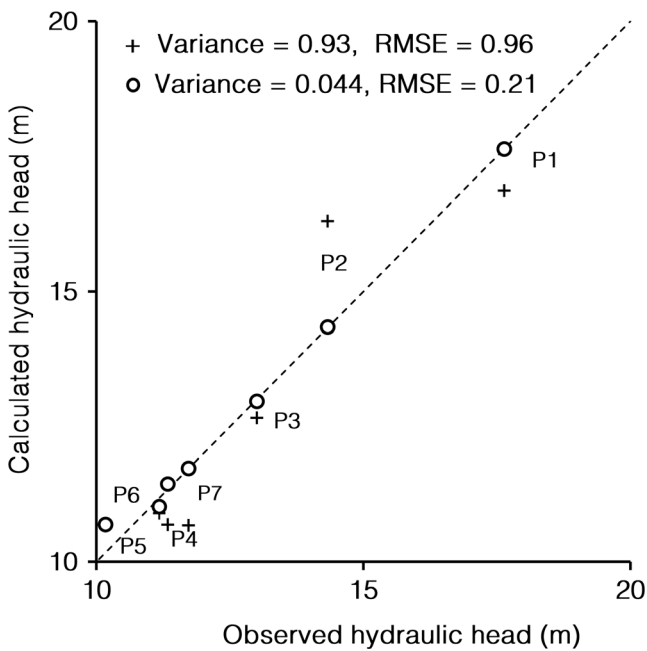| Period	Western hillslope flow (m³/d)		Recharge (m³/d)		Recharge (m³/d)	
	Lower limit	Upper limit	Lower limit	Upper limit	Lower limit	Upper limit
1	99.68	119.04	4.64	34.08	0.49	28.47
2	92.16	115.68	4.64	41.12	−13.60	20.72
3	97.92	125.28	−1.92	39.52	2.53	42.24
4	92.32	112.96	4.32	36.16	−10.25	19.71
5	97.92	117.44	12.96	42.72	7.44	35.60
6	94.88	115.68	6.24	38.40	−14.17	16.10
7	98.56	119.04	7.68	39.20	2.34	32.03

Fig. 10 Comparison between calculated and observed hydraulic heads for each piezometer (*P1–P7*) before (*cross*) and after (*circle*) the calibration

raising the hydraulic head level while river stages remained lower.

The average fluxes estimated by STRIVE are about 25 % of the average estimated by MODFLOW at T2. STRIVE, however, only estimates vertical fluxes, while MODFLOW also includes lateral flow which, under the morphological conditions at T2, can be prevalent.

Conclusions

Results from a groundwater flow model of the alluvial aquifer and vertical aquifer–river exchange fluxes calculated from temperature profiles measured in the Cumbe River show an active exchange of water between the river and the aquifer with both temporal and spatial variation. The morphological conditions surrounding the investigated locations influence the exchange in both cases. Two distinct zones have been identified, a gaining river upstream in the narrower alluvial and more upstream valley, and a losing river downstream in the wider alluvial valley.

The gaining river section is ratified by average values of stream stage (10.65 m) and water-table elevation nearby the stream (11.18 m), both values above to the reference elevation at 2,633.45 m a.s.l. The hydrological connectivity between the hillslopes and the alluvial valley contributes to the storage of water in the alluvial aquifer; 92 % of flow into the alluvial deposits originates from lateral flow coming from the hillslopes.

The losing river section is found in the open alluvial valley where the water table is notably less influenced by hillslope flows. Although this section is investigated using only temperature as the groundwater tracer, it can be concluded that the wider downstream alluvial plain, with relatively limited slope, buffers the dynamics of the river and the alluvial storage. The variable conditions of GW–SW interaction, and changes in flow direction from losing to gaining, are indicated and justify future similar investigations in the upstream section.

The interaction of the hillslope with the upstream alluvial valley leads to a prevalent lateral flow exchange between the
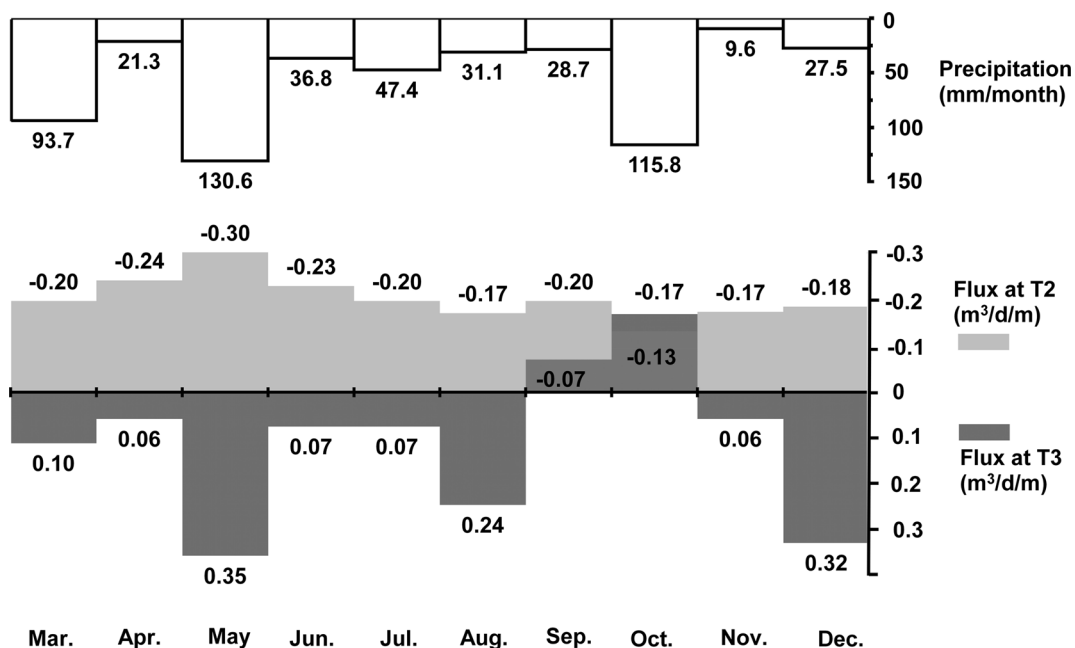

Fig. 11 Water fluxes per meter of river calculated with the STRIVE model from riverbed temperature profiles at *T2* and *T3*; a *negative value* indicates upward flux

aquifer and the river. This is confirmed by comparison between MODFLOW and STRIVE's average flows, since STRIVE estimates 1D vertical flow and MODFLOW the total flow (including lateral flow). The vertical flow calculated with STRIVE is only 25 % of the flow calculated by MODFLOW.

The alluvial plain forms a buffer or transition zone. This allows a gradual flow of runoff coming from the upper hills toward the river, releasing and sustaining water flow into the river. At the eastern side of the Cumbe River a road is present; there, disturbances in the flow contribution from the hillslopes have been detected. For further research, a precise quantification of these disturbances and the influence of the infrastructure with respect to the flow towards the river is recommended.

So far, the contribution of GW–SW interactions and the specific role of the alluvial valley have been ignored in the studied area of the Cumbe and Tarqui River catchments. This work represents the first attempt to investigate GW–SW interaction combining field investigations and modelling techniques.

In the past, human interventions were commonly developed while ignoring GW–SW interactions and its effects in the hydrogeological processes. Future land use planning and development of the city of Cuenca should include concepts presented in this study such as hydrological connectivity, in order to improve the assessment of the sustainability of the catchment water resources and preservation of its aquatic ecosystems.

References

Amoros C, Bornette G (2002) Connectivity and biocomplexity in waterbodies of riverine floodplains. Freshw Biol 47:761–776. doi:10.1046/j.1365-2427.2002.00905.x

Anderson M (2005) Heat as a ground water tracer. Ground Water 43:951–968. doi:10.1111/j.1745-6584.2005.00052.x

Anibas C, Buis K, Getatchew A et al (2008) Determination of groundwater fluxes in the Belgian Aa River by sensing and simulation of streambed temperatures. IAHS Publ Ser Proc Rep 321, IAHS, Wallingford, UK, pp 46–53

Anibas C, Fleckenstein J, Volze N et al (2009) Transient or steady-state? Using vertical temperature profiles to quantify groundwater–surface water exchange. Hydrol Process 23:2165–2177. doi:10.1002/hyp.7289

Anibas C, Buis K, Verhoeven R et al (2011) A simple thermal mapping method for seasonal spatial patterns of groundwater–surface water interaction. J Hydrol 397:93–104. doi:10.1016/j.jhydrol.2010.11.036

Anibas C, Verbeiren B, Buis K et al (2012) A hierarchical approach on groundwater–surface water interaction in wetlands along the upper Biebrza River, Poland. Hydrol Earth Syst Sci 16:2329–2346. doi:10.5194/hess-16-2329-2012

Barberi F, Coltelli M, Ferrara G et al (1988) Plio-Quaternary volcanism in Ecuador. Geol Mag 125:1–14. doi:10.1017/S0016756800009328

Bracken L, Croke J (2007) The concept of hydrological connectivity and its contribution to understanding runoff-dominated geomorphic systems. Hydrol Process 21:1749–1763. doi:10.1002/hyp.6313

Broekaert S (2012) Land use dynamics and the spatial occurrence of shallow landslides in a tropical mountainous catchment, Ecuador. KU Leuven, Leuven, The Netherlands

Brunke M, Gonser T (1997) The ecological significance of exchange processes between rivers and groundwater. Freshw Biol 37:1–33. doi:10.1046/j.1365-2427.1997.00143.x

Buytaert W, Beven K (2011) Models as multiple working hypotheses: hydrological simulation of tropical alpine wetlands. Hydrol Process 25:1784–1799. doi:10.1002/hyp.7936

Buytaert W, De Bièvre B, Wyseure G, Deckers J (2004) The use of the linear reservoir concept to quantify the impact of changes in land use on the hydrology of catchments in the Andes. Hydrol Earth Syst Sci 8:108–114. doi:10.5194/hess-8-108-2004

Buytaert W, Deckers J, Wyseure G (2006) Description and classification of nonallophanic Andosols in south Ecuadorian alpine grasslands (páramo). Geomorphology 73:207–221. doi:10.1016/j.geomorph.2005.06.012

Chiang W-H, Kinzelbach W (1998) Processing MODFLOW: a simulation system for modeling groundwater flow and pollution. http://www.hydrogm.uni-jena.de/hydrogmmedia/LectureMaterial/Material+2015+Transport/Handbuch+zu+Processing+Modflow.pdf. Accessed December 2015

Constantz J (2008) Heat as a tracer to determine streambed water exchanges. Water Resour Res 44:W00D10. doi:10.1029/2008WR006996

Dahm CN, Grimm NB, Marmonier P et al (1998) Nutrient dynamics at the interface between surface waters and groundwaters. Freshw Biol 40:427–451. doi:10.1046/j.1365-2427.1998.00367.x

Datry T, Larned ST, Scarsbrook MR (2007) Responses of hyporheic invertebrate assemblages to large-scale variation in flow permanence and surface–subsurface exchange. Freshw Biol 52:1452–1462. doi:10.1111/j.1365-2427.2007.01775.x

De Smedt F, Yongbo L, Gebremeskel S (2000) Hydrologic modelling on a catchment scale using GIS and remote sensed land use information. In: Brebbia CA (ed) 2000, Risk Analysis II, WIT, Boston, MA, pp 295–304

De Vries DA (1963) Thermal properties of soils. In: van Wijk WD (ed) Physics of plant environment. North-Holland, Amsterdam, pp 210–235

Ellis PA, Mackay R, Rivett MO (2007) Quantifying urban river–aquifer fluid exchange processes: a multi-scale problem. J Contam Hydrol 91:58–80. doi:10.1016/j.jconhyd.2006.08.014

Gibert J, Danielopol D, Stanford JA (1994) Groundwater ecology. Academic, San Diego

Guzmán P, Batelaan O, Huysmans M, Wyseure G (2015) Comparative analysis of baseflow characteristics of two Andean catchments. Ecuador Hydrol Process 29(14):3051–3064. doi:10.1002/hyp.10422

Hancock PJ, Boulton AJ, Humphreys WF (2005) Aquifers and hyporheic zones: towards an ecological understanding of groundwater. Hydrogeol J 13:98–111. doi:10.1007/s10040-004-0421-6

Harbaugh AW (2005) MODFLOW-2005, the US Geological Survey modular ground-water model: the ground-water flow process. US Geological Survey, Reston, VA

Harbaugh AW, Banta ER, Hill MC, McDonald MG (2000) MODFLOW-2000, the US Geological Survey modular ground-water model: user guide to modularization concepts and the ground-water flow process. US Geological Survey, Reston, VA

Holmes RM (2000) The importance of ground water to stream ecosystem function. Streams Ground Waters 2000:137–148. doi:10.1016/B978-012389845-6/50006-5

Hungerbühler D, Steinmann M, Winkler W et al (2002) Neogene stratigraphy and Andean geodynamics of southern Ecuador. Earth-Sci Rev 57:75–124. doi:10.1016/S0012-8252(01)00071-X

Kalbus E, Reinstorf F, Schirmer M (2006) Measuring methods for groundwater–surface water interactions: a review. Hydrol Earth Syst Sci 10:873–887. doi:10.5194/hess-10-873-2006

Lane SN, Brookes CJ, Kirkby MJ, Holden J (2004) A network-index-based version of TOPMODEL for use with high-resolution digital topographic data. Hydrol Process 18:191–201. doi:10.1002/hyp.5208

Lapham WW (1989) Use of temperature profiles beneath streams to determine rates of vertical ground-water flow and vertical hydraulic conductivity. US Geol Surv Water Suppl Pap 2337

Liu YB, De Smedt F (2004) WetSpa extension, a GIS based hydrologic model for flood prediction and watershed management. Documentation and user manual. Vrije Univ, Brussels, Belgium, 108 pp

Pretty JL, Hildrew AG, Trimmer M (2006) Nutrient dynamics in relation to surface–subsurface hydrological exchange in a groundwater fed chalk stream. J Hydrol 330:84–100. doi:10.1016/j.jhydrol.2006.04.013

Pringle C (2003) What is hydrologic connectivity and why is it ecologically important? Hydrol Process 17:2685–2689. doi:10.1002/hyp.5145

Ritzema HP (1994) Drainage principles and applications, 2nd edn. International Institute for Land Reclamation and Improvement, Wageningen, The Netherlands

Smith JWN (2005) Groundwater-surface water interactions in the hyporheic zone. Environment Agency Science report SC030155/1, Environment Agency, Bristol, UK

Soetaert K, DeClippele V, Herman P (2002) FEMME, a flexible environment for mathematically modelling the environment. Ecol Model 151:177–193. doi:10.1016/S0304-3800(01)00469-0

Sophocleous M (2002) Interactions between groundwater and surface water: the state of the science. Hydrogeol J 10:52–67. doi:10.1007/s10040-001-0170-8

Soulsby C, Malcolm I, Youngson A (2001) Hydrochemistry of the hyporheic zone in salmon spawning gravels: a preliminary assessment in a degraded agricultural stream. Regul Rivers Res Manag 17:651–665. doi:10.1002/rrr.625

Stallman RW (1965) Steady one-dimensional fluid flow in a semi-infinite porous medium with sinusoidal surface temperature. J Geophys Res 70:2821–2827. doi:10.1029/JZ070i012p02821

Tetzlaff D, Soulsby C, Bacon PJ et al (2007) Connectivity between landscapes and riverscapes: a unifying theme in integrating hydrology and ecology in catchment science? Hydrol Process 21:1385–1389. doi:10.1002/hyp.6701

Wang Z-M, Batelaan O, De Smedt F (1996) A distributed model for water and energy transfer between soil, plants and atmosphere (WetSpa). Phys Chem Earth 21:189–193. doi:10.1016/S0079-1946(97)85583-8

Watermark Computing (2004) PEST: model-independent parameter estimation, 5th edn. Watermark, Brisbane, Australia

Winter TC, Harvey JW, Franke OL, Alley WM (1999) Ground water and surface water: a single resource. DIANE, Denver, CO

Woessner WW (2000) Stream and fluvial plain ground water interactions: rescaling hydrogeologic thought. Ground Water 38:423–429. doi:10.1111/j.1745-6584.2000.tb00228.x

Wroblicky GJ, Campana ME, Valett HM, Dahm CN (1998) Seasonal variation in surface–subsurface water exchange and lateral hyporheic area of two stream–aquifer systems. Water Resour Res 34:317–328. doi:10.1029/97WR03285